IACMI/R0008-2018/3.5

Enabling Composite Processing through the OEM Assembly Line

Authors:

Brian Okerberg, PPG
Kar Tean Tan, PPG
Mahmood Haq, MSU

Date: 2-27-2018

Final Technical Report
PA16-0349-3.5-01

Approved for Public Release.
Distribution is Unlimited.

The Institute for iacmi Advanced Composites Manufacturing Innovation
THE COMPOSITES INSTITUTE

U.S. DEPARTMENT OF ENERGY

DOCUMENT AVAILABILITY

Reports produced after January 1, 1996, are generally available free via US Department of Energy (DOE) SciTech Connect.

Website http://www.osti.gov/scitech/

Reports produced before January 1, 1996, may be purchased by members of the public from the following source:

National Technical Information Service
5285 Port Royal Road
Springfield, VA 22161
Telephone 703-605-6000 (1-800-553-6847)
TDD 703-487-4639
Fax 703-605-6900
E-mail info@ntis.gov
Website http://www.ntis.gov/help/ordermethods.aspx

Reports are available to DOE employees, DOE contractors, Energy Technology Data Exchange representatives, and International Nuclear Information System representatives from the following source:

Office of Scientific and Technical Information
PO Box 62
Oak Ridge, TN 37831
Telephone 865-576-8401
Fax 865-576-5728
E-mail reports@osti.gov
Website http://www.osti.gov/contact.html

Acknowledgment: "The information, data, or work presented herein was funded in part by the Office of Energy Efficiency and Renewable Energy (EERE), U.S. Department of Energy, under Award Number DE-0006926."

Final Technical Report

Project Title: Enabling Composite Processing through the OEM Assembly Line
Project Agreement: PA16-0349-3.5-01
Project Period: 01:2017 – 09/2017

Principal Investigator	PPG	PPG	MSU
Name	Brian Okerberg	Kar Tean Tan	Mahmood Haq
Phone number	okerberg@ppg.com	Kartean.tan@ppg.com	haqmahmo@egr.msu.edu
Email	412-492-5259	412-492-5403	517-355-2250

PPG Industries, Inc.
4325 Rosanna Drive
Allison Park, PA 15101

Michigan State University
Department of Civil and Environmental Engineering
3569 Engineering Building, East Lansing, MI 48824

January 23, 2018

Prepared by:
Institute for Advanced Composites Manufacturing Innovation
Knoxville, TN 37932
Managed by Collaborative Composite Solutions, Inc.
For the
U.S. DEPARTMENT OF ENERGY
Under contract DE- EE0006926

Project Period:
(01/2017 – 09/2017)

Approved For Public Release

TABLE OF CONTENTS

1. LIST OF ACRONYMS

DOE: Department of Energy
AMO: Advanced manufacturing Office
OEM: Original Equipment Manufacturer
FRP: Fiber Reinforced Panel
CFRP: Carbon Fiber Reinforced Panel
CTE: Coefficient of Thermal Expansion
HHS: High Hardened Steel
WCA: Water Contact Angle
UVO: Ultraviolet Ozone
UV: Ultraviolet
SEM: Scanning Electronic Microscope
CSR: Cold Rolled Steel
Al: Aluminum
DI: Deionized
TGA: Thermal Gravimetric Analysis
DCB: Dual Cantilever Beam
DAR: Double Acetone Rubs
HDG: Hot Dipped Galvanized

2. List of Figures

3. List of Tables

4. EXECUTIVE SUMMARY

This project established the fundamentals of electrocoat and structural adhesive bonding of automotive composites to enable composite-to-metal bonding through the automotive OEM assembly line. Results include an understanding of surface preparation and adhesive curing requirements for CFRP to produce strong durable structural composite bonds.

5. INTRODUCTION

An automotive assembly line is an efficient, high-throughput process comprising the press shop, the body shop, and paint shop for the body-in-white, followed by assembly of interior components, and then final marriage to the power train. Currently, the typical bake temperature for an automotive quality e-coat is ~180°C and structural adhesives are co-cured in the oven. To implement CFRP with the current matrix materials, we estimate that the electrocoat must cure at 150°C to ensure that no parts experience greater than 180°C. Additionally, a multi-material construction experiences stresses from different coefficients of thermal expansion between the joined materials. These stresses are exacerbated by higher bake temperatures. The project developed adhesives and e-coat that meet OEM specification when baked at temperatures that are compatible with the low cost composites of interest to the OEMs.

PPG Industries, Inc. (PPG) developed new prototype adhesives and coatings that enable OEMs to introduce structural FRP composites in multi-material designs using their existing assembly lines.

6. BACKGROUND

The structural body of a vehicle, as well as the doors, roof, hood, and trunk, are assembled and passed through the paint shop as one unit. The e-coat, adhesives, primer, basecoat, and clear coat processed in the paint shop must be baked to provide corrosion protection, strength, and a durable finish. Currently, the typical bake temperature for an automotive-quality e-coat is ~180°C and structural adhesives are co-cured in the e-coat oven. Standard CFRP matrix materials are capable of sustaining 180°C temperatures; however, the ovens are set to higher temperatures so that thick/heavy metal sections of the body achieve the minimum cure temperature for 17 minutes. By that point, many exterior and thin metal sections experience temperatures in excess of 205°C. More exotic and expensive composite matrix materials would be needed to survive that temperature, which is not economically-feasible for the automotive industry. Therefore, to implement CFRP with the current matrix materials, we estimate that the electrocoat must be capable of curing at 150°C on the heavy metal sections to ensure that no parts experience greater than 180°C. Another issue that arises from a multi-material construction is the stresses and resulting failures that can be caused by different coefficients of thermal expansion (CTE) between the substrate materials. These stresses are exacerbated by higher bake temperatures. The new adhesives and e-coat designed for composites and multi-material designs will enable economically-viable implementation of the new composites that IACMI is advancing into the automotive industry.

7. RESULTS AND DISCUSSION

Task 1: Benchmark developmental low-cure adhesives

Subtask 1.1: Similar material joints
Goal: Map which adhesive formulas provide a suitable bond for each substrate type.

Activities: PPG's developmental low-cure adhesives and a commercial control will be analyzed in joints of similar substrates. Variables to be studied include substrate (carbon fiber composites, aluminum, high strength steel, and traditional steel), substrate surface preparation, adhesive formula, and cure temperature. Different joining methods will also be evaluated, as recommended by An OEM and the institute. Joined assemblies will be tested for bond durability, lap shear, impact resistance, and T-peel at PPG. Additional characterization of the joint will be done at the institute.

Milestone 1.1: At least one adhesive formula for each substrate of interest will be selected for the gap analysis of Subtask 1.2 based on highest performance against the Subtask 1.1 tests.

Subtask 1.2: Multi-material joints
Goal: Perform gap analysis for developmental low-cure adhesives for composite joints
Activities: PPG's developmental low-cure adhesives and a commercial control will be analyzed in dissimilar joints using the same variables as in 1.1. Adhesive selection will be aided by task 1.1 findings. Joined assemblies will be tested for bond durability, lap shear, impact resistance, and T-peel at PPG. Additional characterization of the joint will be done at the institute.

Milestone 1.2: Gap analysis of developmental adhesive vs. the OEM test specifications tested in Subtask 1.2 for bond durability, lap shear, impact resistance and T-peel for a composite joined to itself, steel, HSS, and aluminum is complete and the quantified magnitude of improvement needed for each test is determined.

DISCUSSION: Adhesives Theoretical Framework

Materials: The adhesive used was a 1K structural adhesive. Two different cure temperatures were employed, including a low bake temperature at 145ºC and a high bake temperature at 180ºC for 10 minutes. The heating rates varied with the types of joints and substrates used due to their differences in thermal inertia. In order to ensure the joints reached the intended temperature and baked for the required duration, a thermocouple was inserted as close as possible to the adhesive layer to monitor its temperature during the bake cycle. The actual cure time was then determined from the moment the adhesive reached the intended temperature.

The substrates used were an aluminum alloy Al6111-T43, carbon fiber reinforced polymer (CFRP) composite and high strength steel (HSS). Aluminum alloy substrates were coated with a dry-film lubricant (Quaker DryCote® 290) prior to adhesive application and HSS substrates

were coated with FERROCOTE® 61A US. These material are commonly used by automotive OEMs.

Specimen Cleaning: Five cleaning methods were tested for their ability to remove surface contamination (hard water scale and cutting debris) from samples that were prepared with a water-cooled diamond saw. Coupons roughly ~0.5" x 0.5" had their Water contact angles (WCA) measured before (as cut) and after cleaning. There was a visible difference in the appearance of the labeled and unlabeled (appears rougher, duller) surfaces of the panel, all measurements were performed on the label side. With the exception of B2, all protocols ended with three rinses with deionized water and oven drying at 90 °C for 20 minutes.

Cleaning Methods:

- B1 Detergent cleaning: Immersion for 10 minutes at 95 °C in an aqueous solution of Alconox® (0.5% w/w)
- B1w Detergent cleaning followed by wiping 10X with a Wypall®
- B2 Solvent rinsing: Thorough acetone rinse followed by wiping 10X with a Wypall®, air dried
- B3 Alkaline cleaning: Immersion for 10 minutes at room temperature in a NaOH solution of pH ~12.
- B3w Alkaline cleaning followed by wiping 10X with a Wypall®

Inspection using incident light after cleaning showed all methods except B2 removed the visible contamination from the surface. Method B2 had irregular areas of scale/cutting debris remaining. The Table 1 lists the measured water contact angles.

Table 1. Water contact angles of cleaned composite surfaces

Cleaning Methods	Average	Standard Deviation	Coefficient of Variance
	(°)	(°)	(%)
B1 (As Cut)	84.4	8.4	9.9
B1 (Cleaned)	92.9	2.3	2.4
B1w (As Cut)	87.0	10.4	12.0
B1w (Cleaned)	95.1	2.0	2.1
B2 (As Cut)	93.1	5.7	6.2
B2 (Cleaned)	90.2	4.8	5.3
B3 (As Cut)	96.6	3.3	3.4
B3 (Cleaned)	97.3	4.9	5.1
B3w (As Cut)	95.7	2.9	3.0
B3w (Cleaned)	100.3	1.1	1.1

The lack of a control surface to provide a target value for WCA required the methods to be evaluated by their ability to remove surface debris and provide a uniform surface, judged by

the WCA standard deviations. Solvent rinsing was eliminated from consideration due to its inability to remove surface debris. Detergent cleaning with and without wiping reduced the standard deviations of the WCA. Alkaline cleaning alone increased the standard deviation of the WCA, the addition of a wiping step resulted in a decrease.

Method B1w was selected to provide a baseline cleaning for the composite surfaces prior to surface treatment.

UVO Surface Treatment: The UVO surface treatment used was a combination of high intensity pulsed UV light and an oxygen/ozone atmosphere. The UV light was generated by a Xenon® model RC-500 system. The specimens were treated in a chamber that was supplied with flowing ozone. Approximately 0.5" of the labeled end of the samples were wrapped in aluminum foil to avoid etching of the labeling ink. Specimens were placed 0.5" or 1.0" from the window of the lamp to vary the intensity of the UV and treated for up to 10 minutes. The WCA measurements were made directly after the samples were treated. For the samples treated and shipped to PPG for subsequent bonding the specimens were individually wrapped in aluminum foil.

Oxygen Plasma Surface Treatment: A Plasma Science model PS-0500 Plasma Treatment System was used for the treatment process. The labeled ends of the samples were wrapped in the same manner used for UVO treatment. The specimens were placed on a sheet of aluminum foil that had previously been plasma etched for 5 minutes. The treatment chamber was evacuated to a pressure of 0.05 Torr and the forward power setting was 50% of 550W (effective power 275W). Specimens were individually treated for the desired time to assure uniformity of the process. WCA measurements and preparation for shipping were the same as for the UVO treatment.

Contact Angle Measurements: Water contact angles (WCA) were measured using a Krüss model DSA 10 Mk2 Drop Shape Analysis System® equipped with a microliter dosing syringe. HPLC grade water was used to form 3µl sessile drops on the surface of interest, their contact angles were recorded after 15 seconds. Five droplets were measured for each surface.

Scanning Electron Microscopy: Specimens were coated with a thin layer of platinum (~ 1nm) and imaged in a Zeiss EVO® LS 25 electron microscope.

Water Contact Angles of Treated Composite Surfaces: To select the treatment conditions for the UVO and plasma treatments a set of composite specimens ~1" x 3" were first cleaned using method B1w. Treatments were carried out in the UVO and plasma chambers for a range of times for both and two distances for the for the UVO. The water contact angles were measured directly after the treatment. Figure 1 shows the effect of treatment method, time, and distance (UVO).

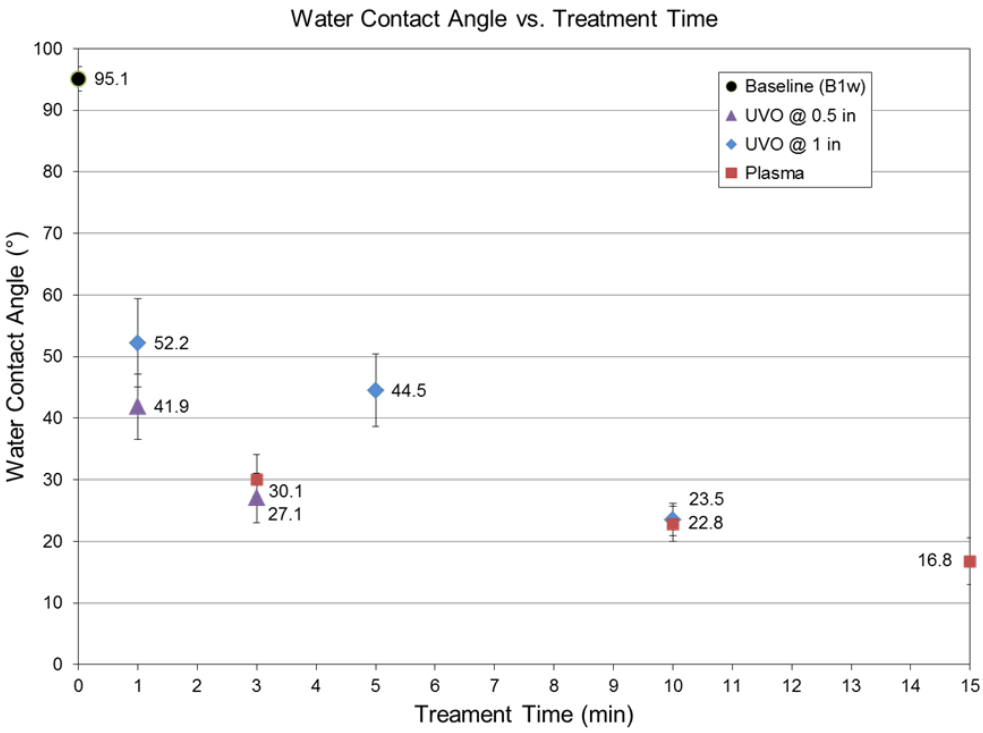

Figure 1. Water contact angle versus treatment time.

Both treatments were effective at reducing the baseline WCA of the composites from the non-wetting regime (WCA ≥ 90°) into the energetically favorable regime (WCA ≤ 90°) for adhesive bonding. An exposure time of 3 minutes was selected for both the plasma and UVO treatment (0.5" distance) for further study.

Scanning Electron Microscopy: The surfaces of the composites were examined after harvesting, cleaning and surface treatment to determine what changes occurred to their morphology. There were two visually distinct areas on the surface of the composites: a generally smooth continuous resin rich field and discrete regions where the fibers were visible. The "as cut" samples had debris adhering on both the resin and fiber rich regions, Figure 2 and Figure 3, respectively. The visual evaluation that the baseline cleaning had removed the surface debris was confirmed by the SEM examination as shown in Figure 4 and Figure 5. The 3 minute plasma treatment did not appreciably alter the appearance of the resin rich areas of the coupons, Figure 6. However, the fiber rich areas did show significant changes, Figure 7. The surface of the fibers became distinct and voids were exposed inside the fiber tows. Figure 8 is a higher magnification view of a portion of the area in Figure 7, the fibers exhibit the longitudinal lines characteristic of a bare fiber surface. The UVO treatment performed in much the same manner as the plasma treatment with regards to changes in the surfaces. The resin rich areas remained appreciably unaltered, Figure 9. The fiber rich areas had enough material removed to expose voids and clean the fiber surfaces, Figure 10 and Figure 11.

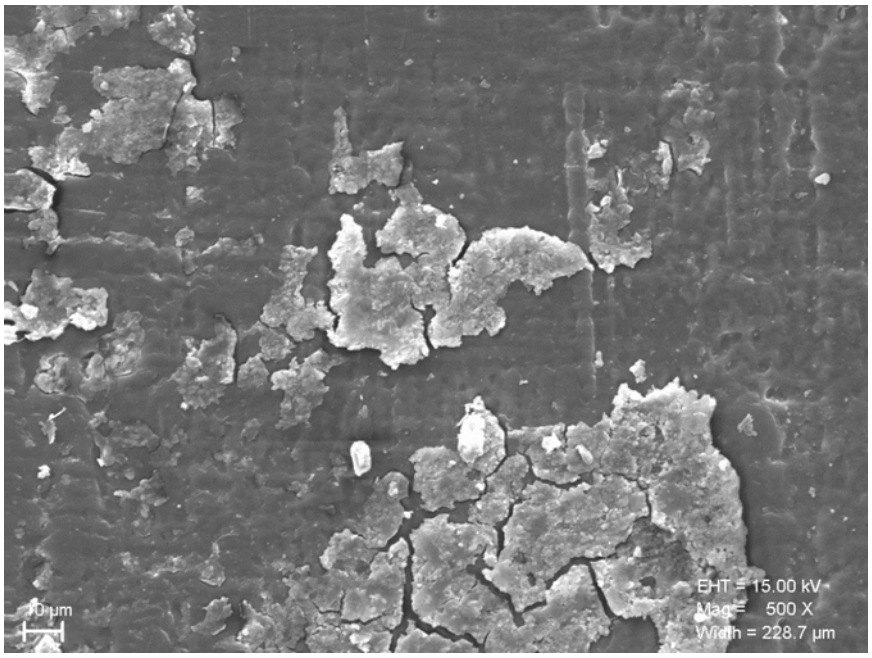

Figure 2. Debris on the surface of an "as cut" coupon, resin rich region.

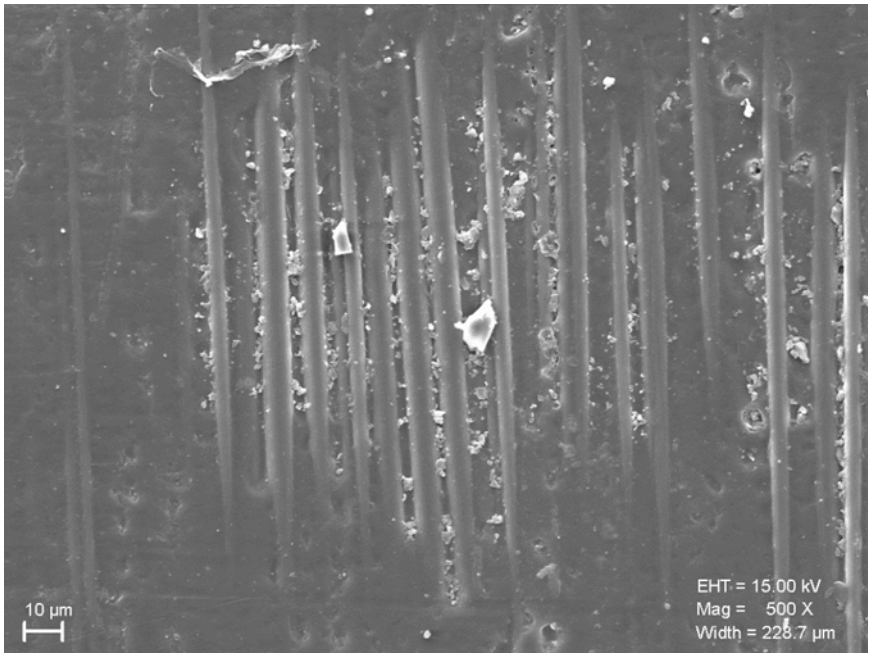

Figure 3. Debris on the surface of an "as cut" coupon, fiber rich region.

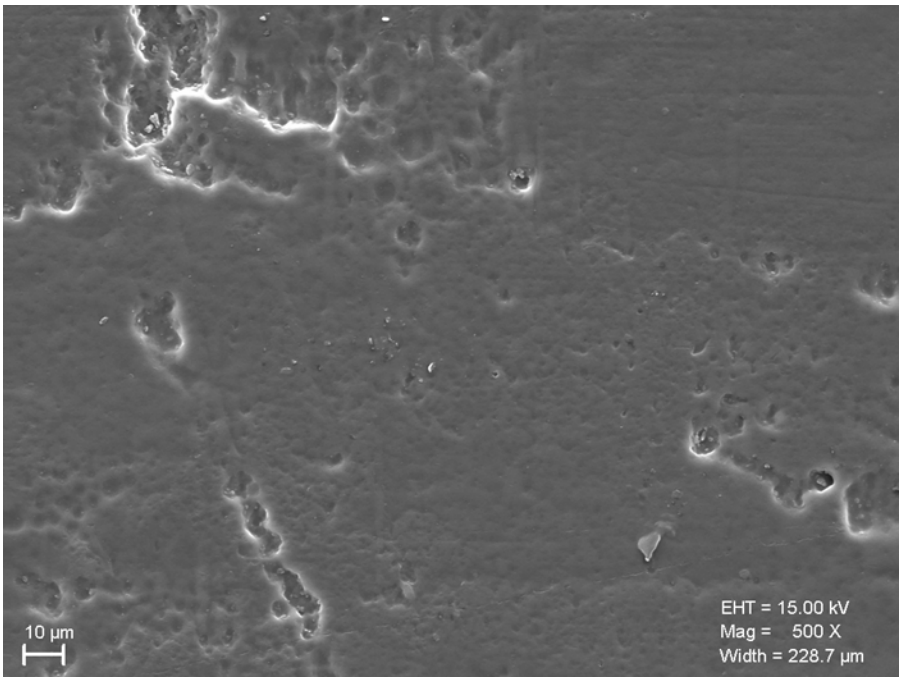

Figure 4. Resin rich region after baseline cleaning.

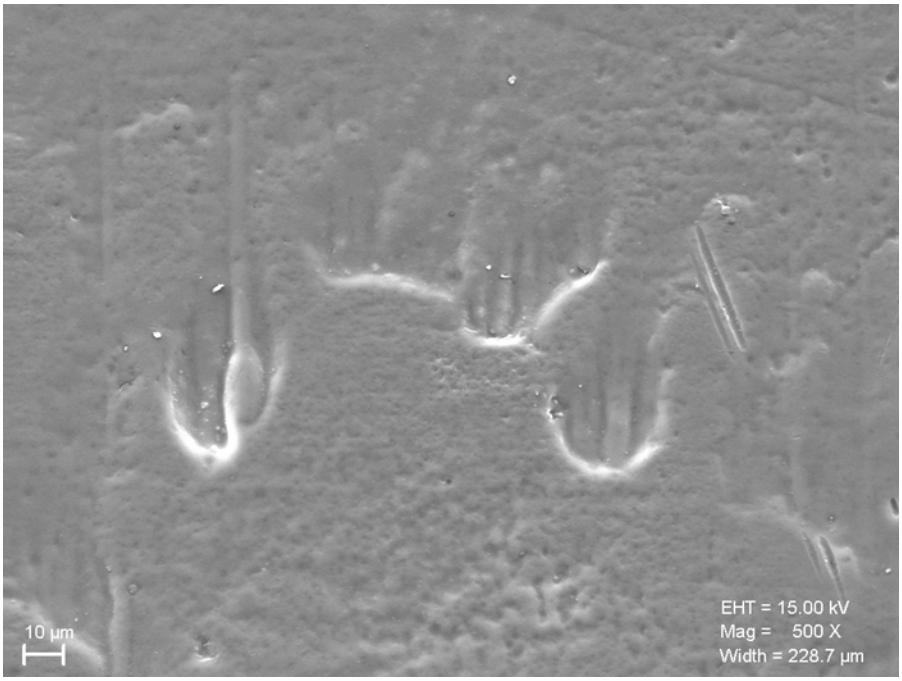

Figure 5. Fiber rich region after baseline cleaning.

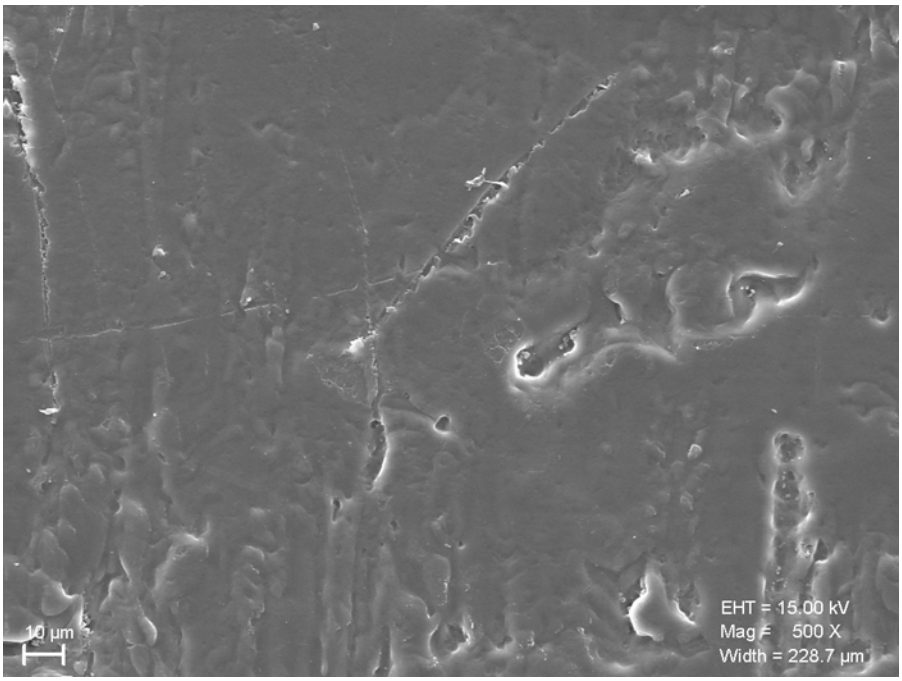

Figure 6. Resin rich area after 3 minutes of treatment with oxygen plasma.

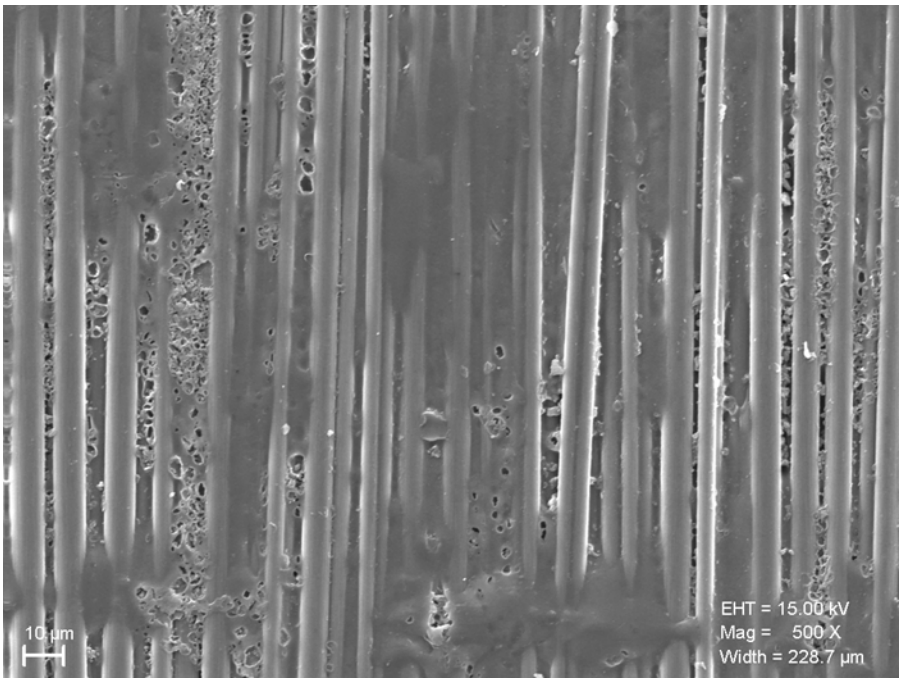

Figure 7. Fiber rich area after 3 minutes of treatment with oxygen plasma.

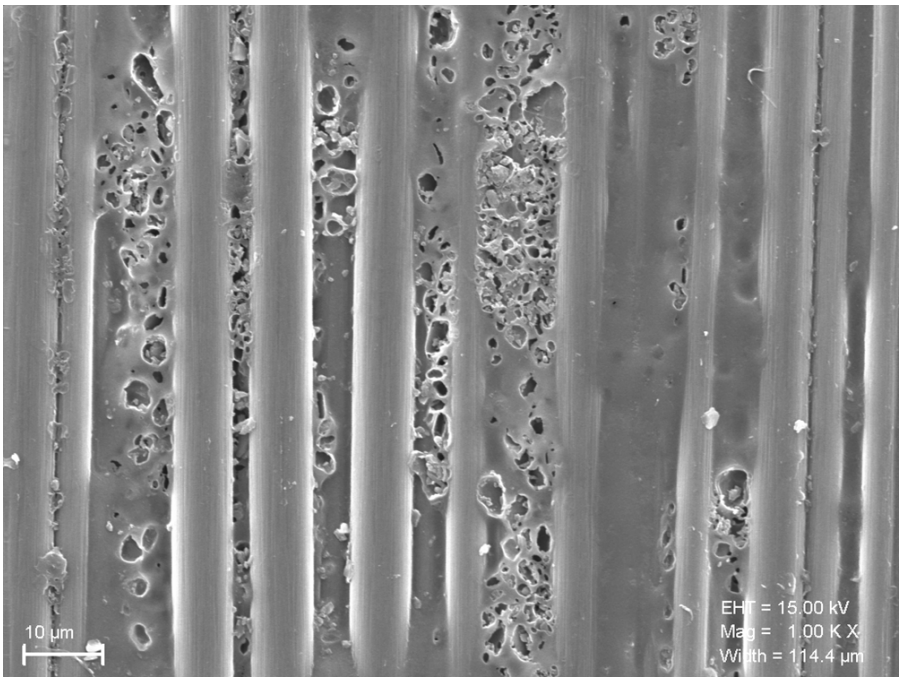

Figure 8. Fiber rich area after 3 minutes of treatment with oxygen plasma, higher magnification.

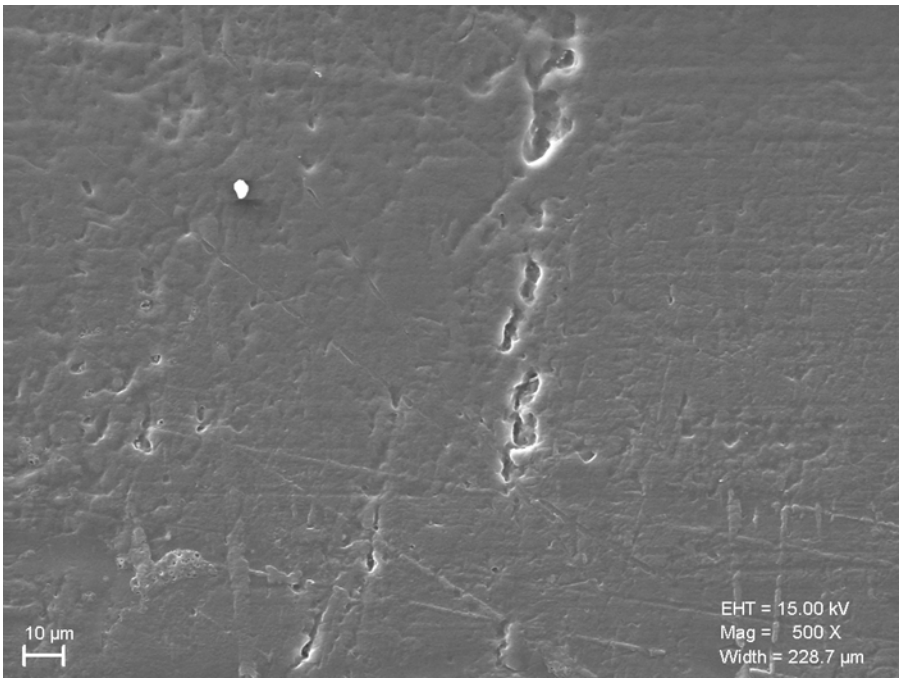

Figure 9. Resin rich area after 3 minutes of treatment with UVO.

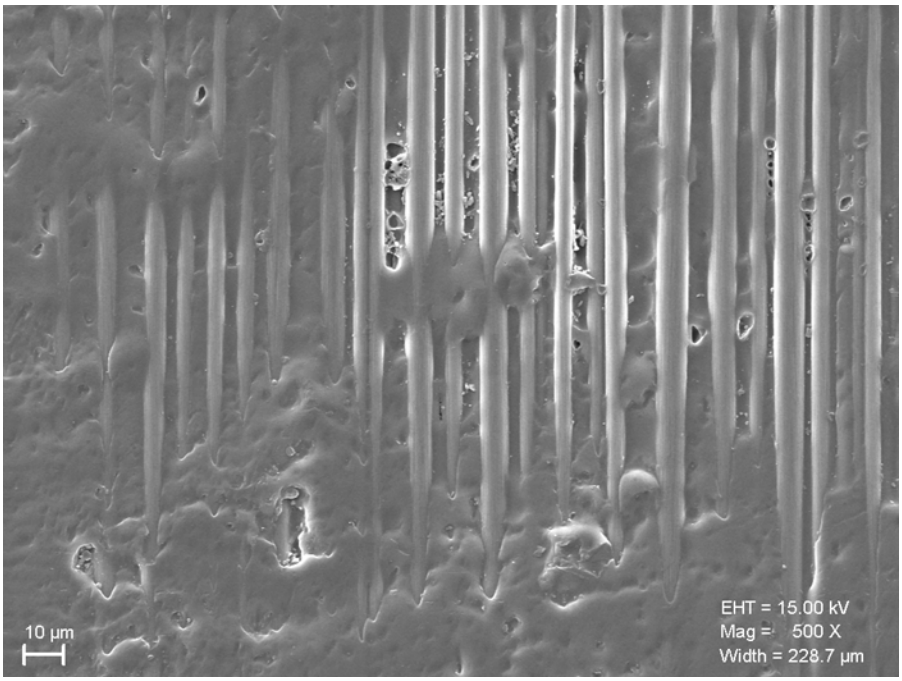

Figure 10. Fiber rich area after 3 minutes of treatment with UVO.

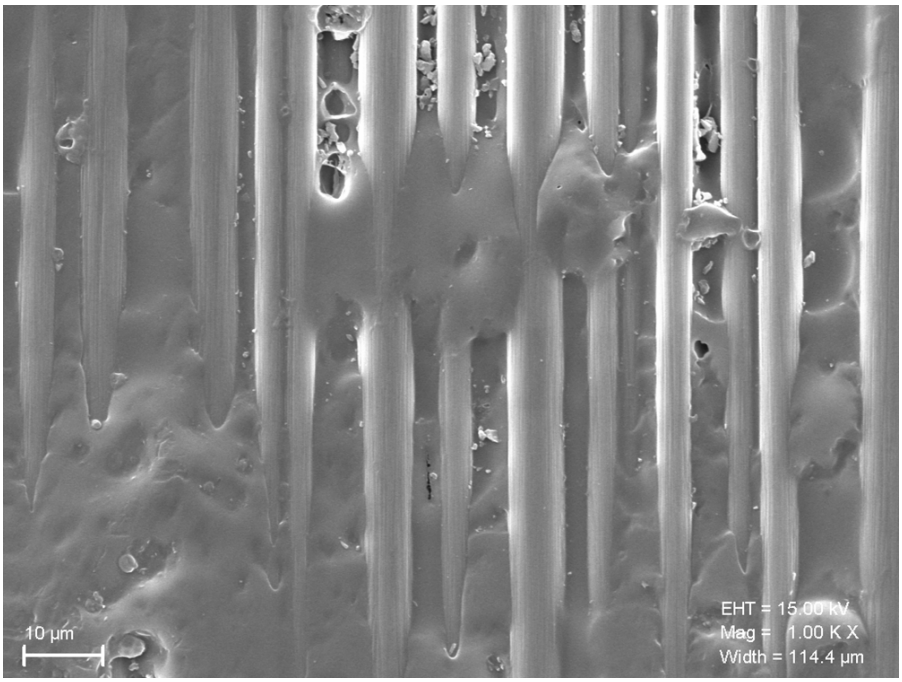

Figure 11. Fiber rich area after 3 minutes of treatment with UVO, higher magnification.

Task 2: Benchmark developmental low-cure e-coat

Subtask 2.1: Standalone panels
Goal: Perform gap analysis for developmental low-cure e-coat over standalone panels of various substrate materials

Activities: PPG's developmental low-cure e-coats and a commercial control will be analyzed over standalone panels of traditional and lightweight substrates. Variables to be studied include substrate type, e-coat formulation, and cure temperature. The remainder of the coating system will be held constant. PPG will test the panels for coating adhesion, cyclic corrosion, appearance of each layer, and samples will be sent for Florida exposure testing.

Milestone 2.1: Gap analysis of developmental e-coat vs. the OEM specifications tested in Subtask 2.1 for coating adhesion, cyclic corrosion, and appearance for the tested substrates is complete and the quantified magnitude of improvement needed for each test is determined.

Subtask 2.2: Joined assemblies
Goal: Perform gap analysis for developmental low-cure e-coat over joined multi-material assemblies

Activities: PPG's developmental low-cure e-coats and a commercial control will be analyzed over joined assemblies. Variables to be studied include substrate type, e-coat formulation, and cure temperature. The adhesive and remainder of the coating system will be held constant. PPG will test the assemblies for coating adhesion, cyclic corrosion, appearance of each layer, and samples will be sent for Florida exposure testing.

Milestone 2.2: Gap analysis of developmental e-coat vs. the OEM specification tested in Subtask 2.2 for coating adhesion, cyclic corrosion, and appearance for the tested substrates is complete and the quantified magnitude of improvement needed for each test is determined.

Milestone 2.3: An analysis of the effect of multi-material substrate combination and electrocoat formulation on corrosion performance is complete, and the relative magnitude of the contribution of each to corrosion is determined.

DISCUSSION Electrocoat Theoretical Framework
The substrates employed in this study were cold-rolled steel (CRS), galvanized high strength steel (HSS), 6111 aluminum (Al), and carbon-fiber composite (CFRP). The materials were commercially available or supplied by an OEM. The CFRP material was a woven fiber type.

To evaluate corrosion, cure, and appearance of the individual materials, test coupons (4"x6") were cut from the supplied stock. The test coupons were cleaned in CK2010LP, an alkaline cleaner commercially available from PPG Industries, Inc. The cleaning process involved 2' of spray application followed by an immersion in DI water and then a DI water spray. Following cleaning, the panels were pretreated with a thin-film pretreatment or zinc phosphate. Zircobond 1.5 (thin film pretreatment, commercially available from PPG Industries, Inc) was applied in immersion for 2' at 80 ^{o}C, followed by a DI spray rinse and then dried with hot air. The zinc phosphate treatment was C700, commercially available from PPG Industries, Inc.

Following the phosphate treatment, the panels were spray rinsed with DI water and dried with hot air.

After cleaning and pretreatment, the panels were electrocoated with a control or a prototype electrocoat. The panels were baked at 175 ºC for 25 minutes or 150 ºC for 13 minutes (10 minutes metal temperature). Following the cure process, panels were evaluated for cure, appearance, and corrosion. Cure was evaluated using double acetone rubs and thermogravimetric analysis (TGA). 2.5 R_a appearance values were collected using an SJ-400 Mitutoyo profilometer. Cyclic corrosion testing was done in automated corrosion cabinets (Autotech).

Overlap coupons were also fabricated using similar and dissimilar materials (Al-Al, HSS-HSS, Al-CFRP, and HSS-CFRP). The coupon design was a 1"x4" coupon attached to a 3.5"x4" baseplate (see Figure 12). Holes were punched in the overlap coupon and baseplate to allow bolts to be attached. Adhesive was applied with either a skip to simulate incomplete adhesive application or with adhesive filling the gap between the two plates (see Figure 13). The adhesive formulation was the same as that used in the low cure adhesive development and contained spacer beads 10 mils in diameter to help keep spacing between plates consistent. During processing through typical pretreatment/electrocoat processes, the plates were held together using polypropylene bolts. Electrocoat was applied by heating the bath to 90°F and passing current through a closed electrical system using the substrate as the cathode and a stainless steel anode. Following electrocoat application, the polypropylene bolts were removed and metal clips were used to hold the plates together in the oven (due to the melting temperature of the bolts). The control paint was baked nominal (175°C/25' total) and the prototype was underbake (150°C/13' Total). Stainless steel nuts, bolts, and wire were used to complete a galvanic coupling between the two plates. Fiber washers were used to isolate the stainless steel from the coupon. Any uncoated parts sections were covered with tape before coupons were put into corrosion testing (with no scribe). All aluminum coupons were placed into G-85 A2 cyclic corrosion test and all steel coupons were placed in the L-467 cyclic corrosion test. Following 6 weeks of cyclic corrosion testing, the overlap coupons were scribed, once in the center of the panel, approximately 1 inch below the top of the panel and a second time as close to the overlap of the two plates as possible. The coupons were placed back into cyclic corrosion testing for another 3 weeks following scribe.

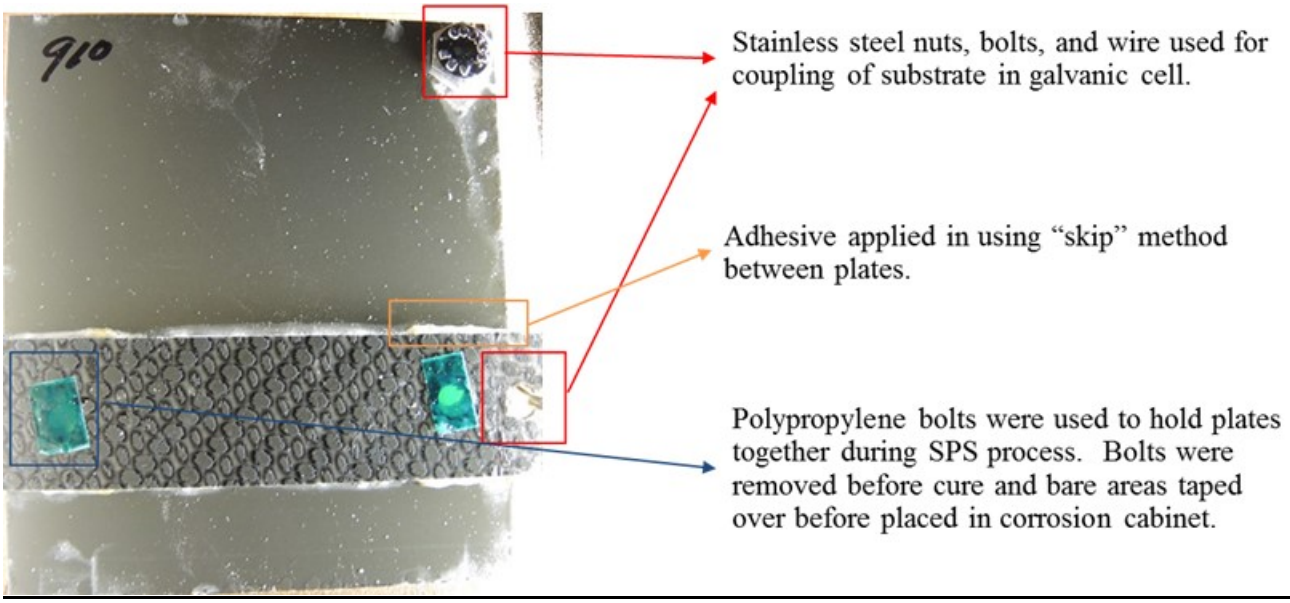

Figure 12: Geometry of the overlap coupons.

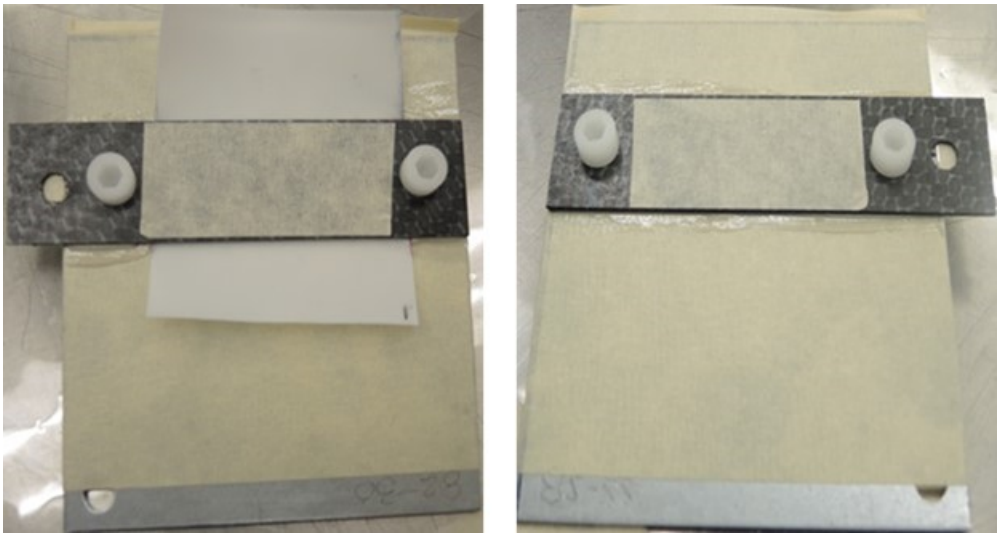

Figure 13: Adhesive was applied with either a skip (left) or no gap between the two plates (right).

8. Benefits Assessment

OEMs will be able to integrate CFRP and other nontraditional materials into the body paint shop process, reducing cost and energy.

9. Commercialization

PPG continues development of the low-cure electrocoat and adhesive technologies. Evaluations are planned when the materials meet published OEM targets for low-temperature materials.

10. Accomplishments

Task 1 Results

Single Lap Shear Tests

Adhesively bonded Al/CFRP joint performance were measured in terms of single lap shear strength and Mode I fracture resistance. The lap shear tests were performed according to ASTM D1002. As show in Figure 14, a single lap shear joint was made by bonding two rectangular substrates (101.6 mm x 25.4 mm) together with an overlap length of 12.7 mm. To reduce eccentric loading path and hence to reduce out-of-plane bending moments, tab ends were bonded on both ends of the samples using a RT cured adhesive. These end tabs were cut from each of the substrate. The adhesive was allowed to cure under ambient conditions for 24h prior to testing. The specimens were tested using a MTS testing machine a nominal crosshead speed of 1.27 mm/min until failure. The peak load and displacement to failure were recorded. Reflective tapes were employed to measure differential displacement between two substrates using a laser extensometer.

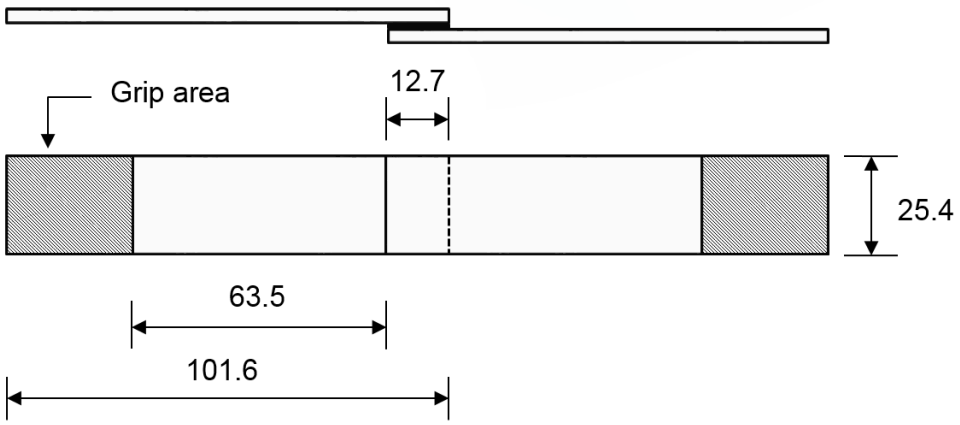

Figure 14. Schematic representation of single a lap shear joint.

Mode I Fracture Tests

Mode I fracture resistance was characterized using a fracture mechanics based test method using double cantilever beam (DCB) specimens (ASTM D5528). The joint configurations included CFRP/CFRP, Al/Al, HSS/HSS, Al/CFRP, Al/HSS and CFRP/HSS. Figure 15 shows the schematic representation of a DCB test specimen. A starter crack with a length of 40 mm

from the edge of the specimen was added to all DCB specimen using 20µm-thick Tedlar insert films. The data reduction method described in ASTM D3433 has been employed to calculate fracture energy from the experimental data using a simple beam theory:

$$G_C = \frac{3P\delta}{2ba}$$

where P is the applied load, δ is the point load displacement, b is the specimen width and a is the crack length which was measured from the loading point. Alternative analysis to capture transverse shear deflection and crack tip rotation has also been developed (Blackman et al. and Williams). To fulfill the linear elastic fracture mechanics requirements, the substrates were reinforced by bonding an auxiliary Al backing substrate to eliminate plastic deformation of the substrates. The backing substrates were bonded using a toughened epoxy adhesive, which was allowed to cure under ambient conditions for 12 hours prior to testing. To facilitate attachment to the testing machine, hinges were bonded and reinforced with a steel/epoxy putty. To monitor the crack growth, one side of the specimen was painted and a marked scale was glued to the specimen.

This test method was adopted instead of T-peel and impact resistance tests outlined in the original work plan because the DCB test allows a direct comparison among various joint configurations, which can be accomplished by matching the bending stiffness of two dissimilar substrates to promote pure Mode I fracture. The ability to make direct comparison is critical as it enables more meaningful baseline evaluation and gap analysis of developmental low cure adhesives.

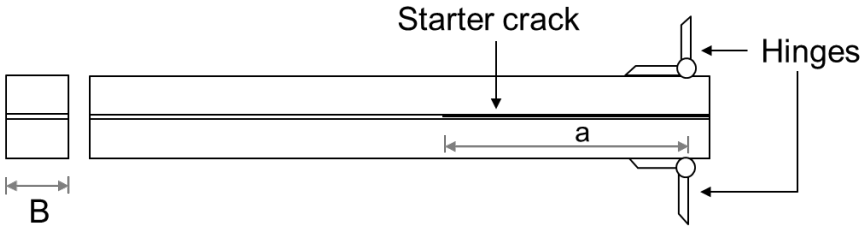

Figure 15. A schematic representation of a DCB specimen.

Lap Shear Peak Loads and Displacements to Failure

Figure 16 shows the peak loads and displacements to failure for all lap shear Al/CFRP joints. The results are also tabulated in Table 2 and Table 3. In the case of 145ºC bake condition, the lap shear strengths for all three different treatments were statistically comparable. Under the 180°C bake condition, the lap shear strength of the clean only joints was the lowest among all different surface preparation methods. The UVO treatment resulted in a similar lap shear strength compared to those of 180ºC bake counterparts. The lap shear strength for the plasma treated joints exhibited an intermediate strength between the clean only and the plasma treated joints. In exception of the UVO treated joints, all joints baked at 180°C displayed a lower strength compared to the 145ºC counterparts. The failure modes for all joints are depicted in Figure 17. The failure mode for the clean only joints baked at 180°C was predominantly

cohesive in the adhesive layer. A mixed failure mode involving cohesive in the adhesive and CFRP interlayer delamination failure was observed for all other joints including UVO and plasma treated joints.

The 145°C cure systems generally displayed larger displacements to failure compared to those of 145°C cure. In particular, UVO and oxygen plasma treatments resulted in the largest displacement to failure, indicating excellent stiffness-toughness balance. The reduction in displacements at high temperature cure (180°C) may be attributed to residual stress effect arising from CTE mismatch between Al and CFRP.

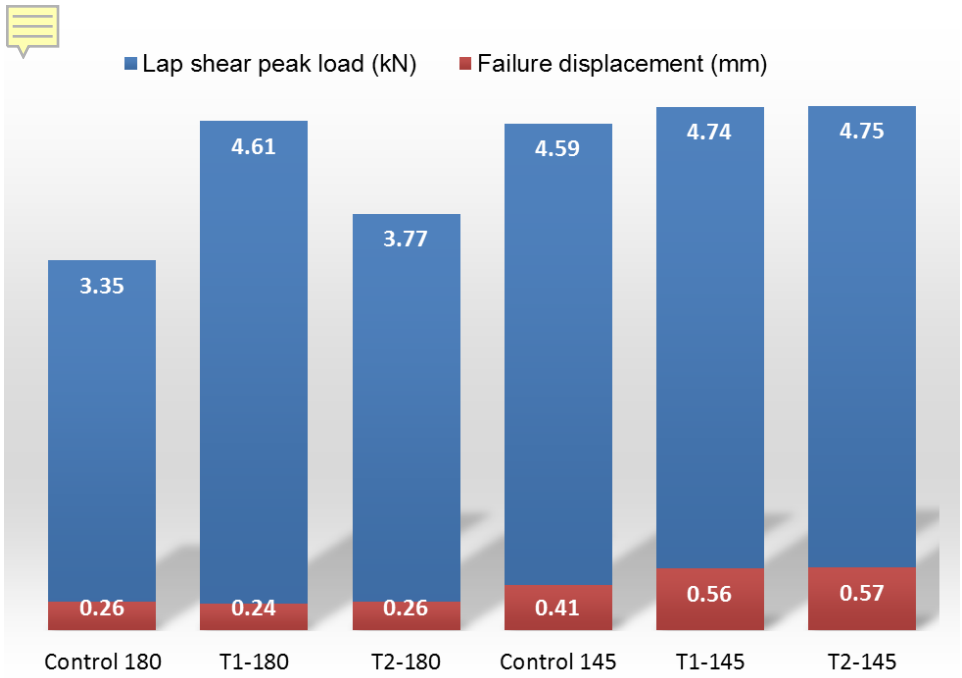

Figure 16. Effect of surface treatments and bake temperatures on Al/CFRP joint performance.

Table 2. Lap shear peak loads for various Al/CFRP joints.

CFRP Surface Preparation	Peak load (N)				Failure Type
	Peak Load	Average	Error +	Error -	
Control 180	3.47	3.35	0.35	0.46	Cohesive
	2.89				Cohesive
	3.70				Cohesive
T1-180 3 min-UVO	4.17	4.61	0.44	0.44	Cohesive
	4.60				Cohesive/Delamination
	5.05				Cohesive/Delamination
T2-180 3 min-oxygen plasma	3.60	3.77	0.35	0.17	Cohesive
	3.60				Cohesive
	4.12				Cohesive/Delamination
Control 145	4.24	4.59	0.44	0.35	Cohesive
	5.03				Cohesive/Delamination
	4.49				Cohesive
T1-145 3 min-UVO	5.20	4.74	0.46	0.51	Delamination
	4.80				Delamination
	4.23				Interfacial/Delamination
T2-145 3 min-oxygen plasma	4.97	4.75	0.22	0.37	Cohesive/Delamination/Interfacial
	4.38				Cohesive/Delamination/Interfacial
	4.89				Cohesive/Delamination/Interfacial

Cohesive – failure occurs within the adhesive bulk leaving even amounts of adhesive on substrate surface, the bond interface is maintained

Interfacial – the adhesive peels from the substrate indicating failure at the adhesive interface

Delamination – the matrix of the composite substrate fails, the bond interface is maintained

Table 3. Lap shear displacements to failure for various Al/CFRP joints.

CFRP Surface Preparation	Displacement to Failure (mm)			
	Displacement	Average	Error +	Error -
Control 180	0.24	0.26	0.02	0.01
	*			
	**			
T1-180 3 min-UVO	**	0.24	0.00	0.00
	0.25			
	0.27			
T2-180 3 min-oxygen plasma	0.3	0.26	0.01	0.01
	0.54			
	0.39			
Control 145	0.69	0.41	0.13	0.11
	**			
	0.43			
T1-145 3 min-UVO	0.61	0.56	0.13	0.13
	0.49			
	0.62			
T2-145 3 min-oxygen plasma	0.24	0.57	0.05	0.08
	**			
	**			

(**) Laser extensometer data at inconclusive due to laser interference from sample surface and/or joint rotation

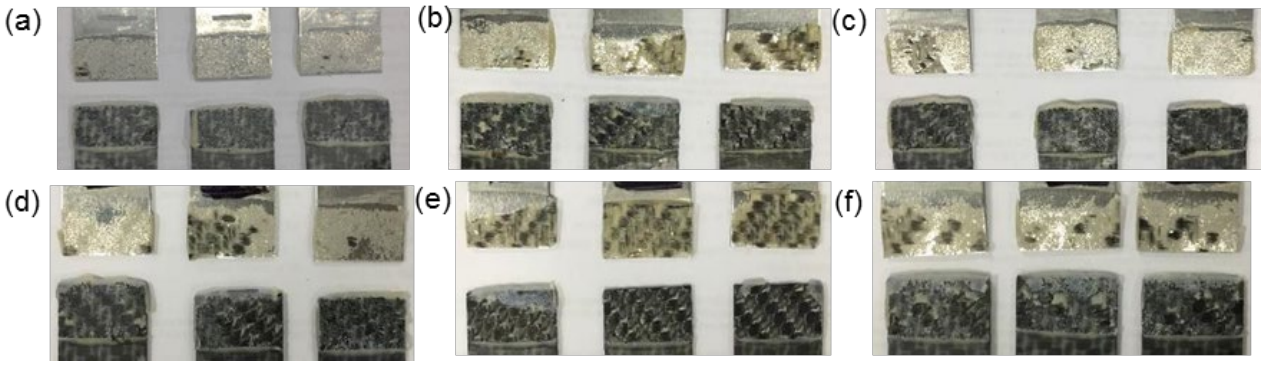

Figure 17. Failure surfaces of Al/CFRP joints.

(a) Control 180; (b) T1–180; (c) T2–180; (d) Control 145; (e) T1-145; (d) T2-145. Control = Cleaning with a mild detergent; T1 = UV/ozone etching; T2 = oxygen plasma etching.

Mode I Double Cantilever Beam Data

The CFRP/CFRP, Al/CFRP and CFRP/HSS, CFRP substrates underwent matrix delamination before failure along the substrate/adhesive interface or cohesively within the adhesive layer. The results imply that the interlaminar fracture strength of CFRP was lower than the Mode I fracture strength of the adhesive/substrate combination. (Figure 18) Therefore, Model I of CFRP specimens showed substrate failure similar to lap shear joints, indicating that the joint strength was stronger than the substrate interlaminar strength.

For samples with Al/Al, Al/CFRP and Al/HSS, the delamination occurred along the Al substrate backing and adhesive before crack data could be obtained. Surface abrasion was the only method employed for preparing the Al surface without affecting the epoxy adhesive. The shear strength for the adhesive used on abraded Al was 2530 psi, which was not enough to overcome the interfacial bond strength or the cohesive strength of the adhesive. These finding show good joints can be achieved with suitable substrate failure, not joint failure.

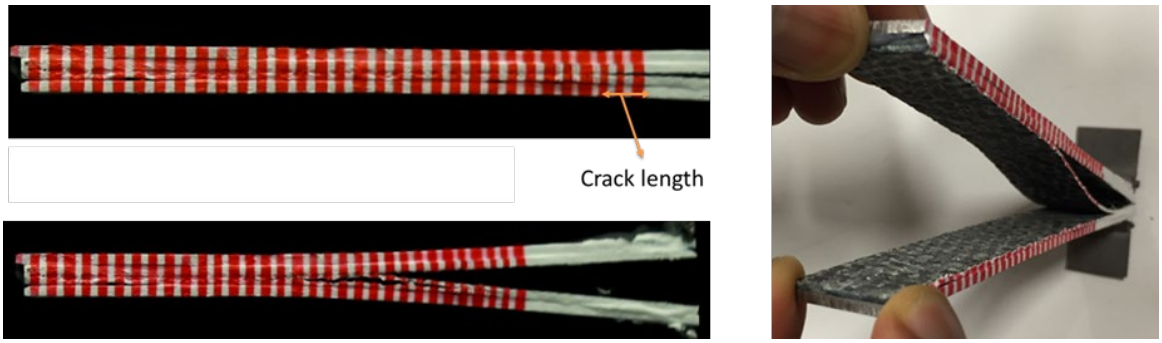

Figure 18. CFRP/CFRP bonded DCB specimen during fracture testing.

Task 2 Results

Standalone Panel Gap Analysis for Low-Cure Electrocoat

The overarching goal of Task #2 was to identify prototype electrocoat formulations that performed within 50% of target value for coating adhesion, cyclic corrosion, appearance, and Florida exposure when baked at 150°C 10 minutes (metal). Evaluation of low-cure prototypes included variations to the polymer backbone and blocking groups on the crosslinker. Candidates were tested for cure (double acetone rubs testing (DAR), thermogravimetric analysis), appearance ($R_{a2.5}$), and corrosion. For stand-alone panels, substrate and pretreatment type had little effect on cure and appearance.

A low cure prototype was selected based on appearance, cure, and corrosion performance on standalone panels. The $R_{a\ 2.5}$ appearance of the low-cure prototype was 83% higher than the control but within the 50% performance limit. The average 2.5 R_a appearance over all substrate and pretreatment types on the control was 0.2 mm and had a DAR rating of 7. The average of the low-cure prototype was 0.3 mm and had a DAR rating of 6. The DAR rating scale is from 1-10, 1 being complete failure to substrate after less than 10 double acetone rubs

and 10 being zero mar after 100 double acetone rubs.

A yellowing study was conducted for the prototype and control electrocoats under five different bake conditions: 150°C/13', 200°C/13', 175°C/28', 150°C/43', and 200°C/43' total cure time. Results showed that oven temperature had a much more significant effect on yellowing than bake time. The yellowing performance of the low-cure prototype was 33% less than the control value.

Thermogravimetric analysis was done on both electrocoats. A constant temperature ramp was used to determine the cure onset temperature which occurred at 152°C for the low cure prototype and 178°C for the control. A three minute ramp to a 150°C/10' isotherm followed by a ramp to 210°C was done to look at weight loss at the cure temperature and the total weight loss. The weight loss as a % of total weight loss was 83.1% for the low cure prototype and 45.5% for the control. The total weight loss was 16.0% for the low cure prototype and 13.4% for the control.

6 weeks G85-A2 cyclic corrosion standalone panels were evaluated. The matrix included three substrates (Al, CRS, and HDG), two electrocoats (low cure prototype and control), two pretreatments (phosphate and thin film), and two cure conditions (150°C/13' total for the low cure system and 175°C/25' total for the control) with duplicate panels for each set of variables. A comparison of the average scribe creep in mm on steel and average filiform corrosion in mm on aluminum is outlined in Table #1 reported as a % of the difference between the two electrocoats (i.e. gap analysis). Pictures of scribe creep, white rust, and filiform corrosion for each variable can be seen in Figure 19. Any number less than 100 indicate that the goal of being within 50% performance of the control was achieved.

Electrocoat adhesion to substrate was measured using a 2mm bearclaw scribe tool. The electrocoats, substrates, pretreatments, and curing conditions tested were the same used for corrosion testing. Electrocoat only adhesion was 100% on all variables tested. Panels with the same variables were prepared for Florida exposure testing. These 4x12 in. panels were sprayed with solvent-borne decorative system (primer, base, and clear). Exposure performance will be recorded every three months for CRS and every 6 months for aluminum and HDG. Gap analysis for standalone panels is summarized in Table 4.

Table 4. Summary of gap analysis of low cure electrocoat prototype compared to the control.

			Cure	Appearance	Adhesion	Corrosion	Exposure
GAP	Al6111T43	PO_4	PASS	36	0	36	IN PROGRESS
	CRS			82	0	60	
	HDG			17	0	33	
	Al6111T43	TFPT		40	10	96	
	CRS			42	0	10	
	HDG			86	0	5	

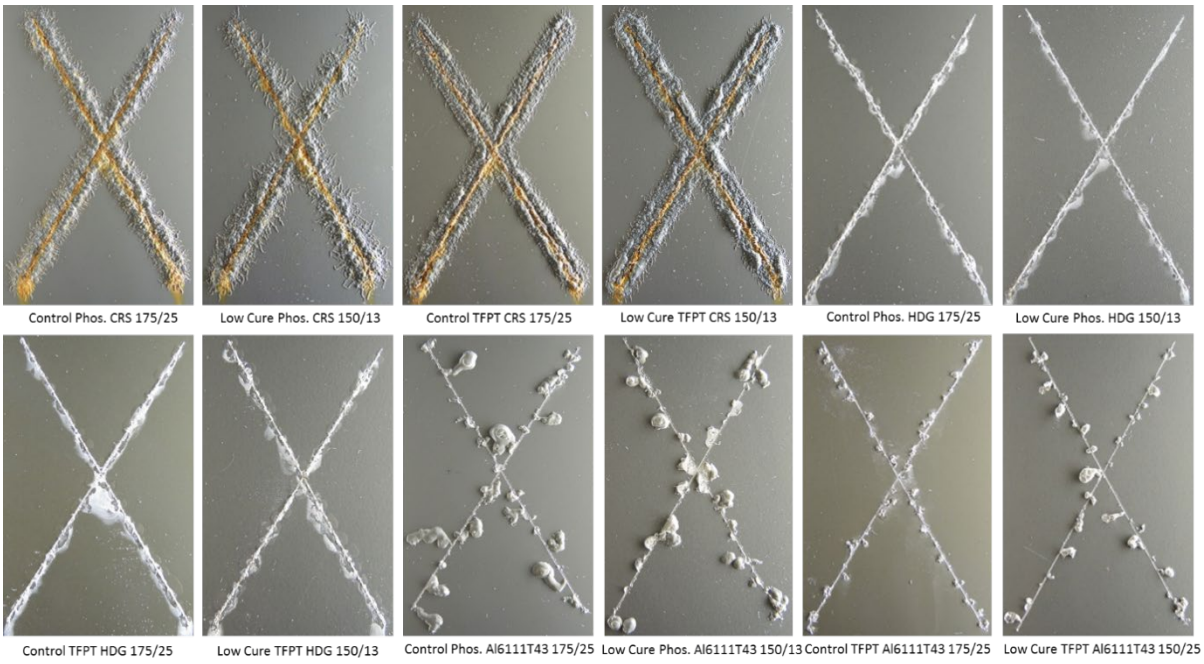

Figure 19.: Pictures of scribe creep, white rust, and filiform corrosion.

For each variable after 6 weeks G85A2 (aluminum substrate) and L467 (steel substrate) cyclic corrosion testing.

Multi-material Joint Gap Analysis for Low-Cure Electrocoat

The carbon fiber was used to test galvanic corrosion performance. The electrocoat did not deposit uniformly on the CFRP. Resin-rich areas appeared to have little coating, while fiber rich areas had significant deposition. Cross-hatch adhesion testing of the e-coated CFRP pieces revealed poor adhesion of the electrocoat. Future evaluations may include treating or cleaning the surface before deposition.

Overlap coupons came out of G85 A2 and L467 corrosion testing for 3-week evaluation. There was evidence of some corrosion at the overlap areas on only a few of the coupons. Individual pictures were taken of each of the coupons and put back into test for an addition 3 weeks. Overlap coupons were removed from corrosion testing for 6-week evaluation. Coupons with full adhesive application did not have any visible corrosion between or around the overlap area. Coupons with skip adhesive had either filiform or rust corrosion mostly around the edge of the panels in the overlap area.

Figure 20 and Figure 21 show examples of overlap coupons following corrosion testing and disassembly. The disassembled plates were sand blasted to help remove residue. Qualitative analysis shows that panels with an adhesive skip had incomplete and non-uniform coverage. Corrosion appeared to be slightly worse in the mixed-metal configuration. There was little difference in the low-cure prototype and control sample. There was significant galvanic corrosion near the connection points.

A separate set of overlap coupons, which were not disassembled following initial corrosion testing, were scribed near the top and near the overlap area, and placed back into test to gather scribe creep data.

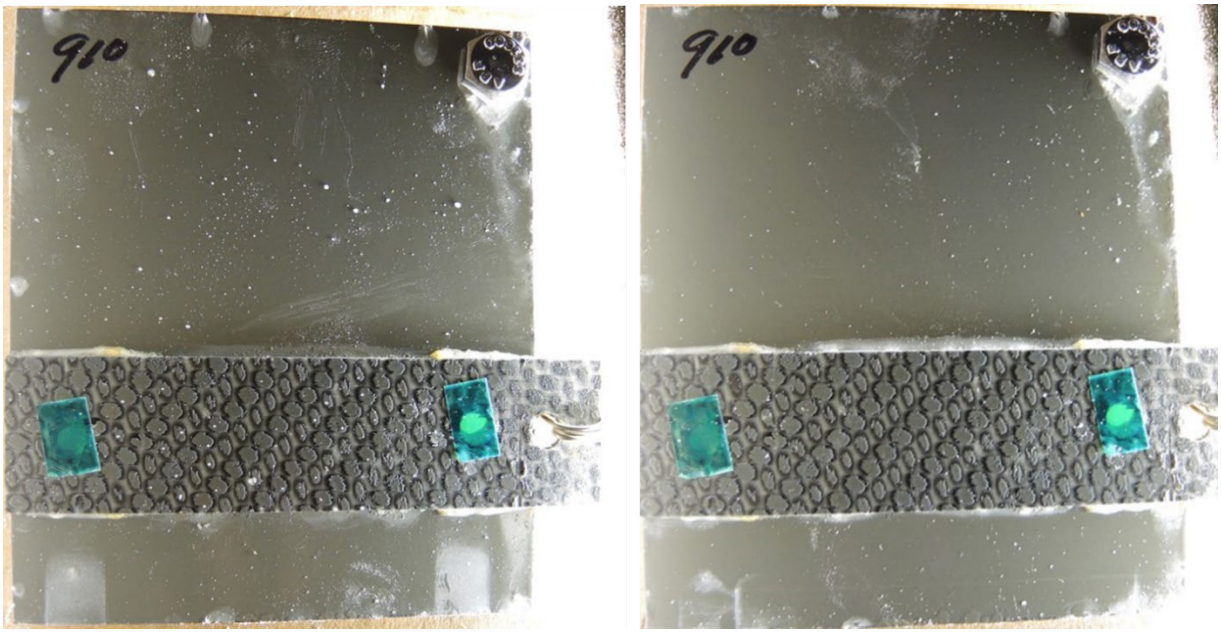

Figure 20. An overlap coupon after 3-weeks (left) and 6-weeks (right) L467 corrosion testing.

The base plate is high strength steel and the front plate substrate is CFRP. Thin film pretreatment, control electrocoat, and skip adhesive application were used.

One obstacle of the overlap coupons in this study was the difference in coefficient of thermal expansion (CTE) between the CFRP and the other substrates. The test coupons had inconsistent spacing between the two plates, which resulted in different spacing between the top plate and the base plate. Optimization of the coupon geometry would be useful for future evaluations.

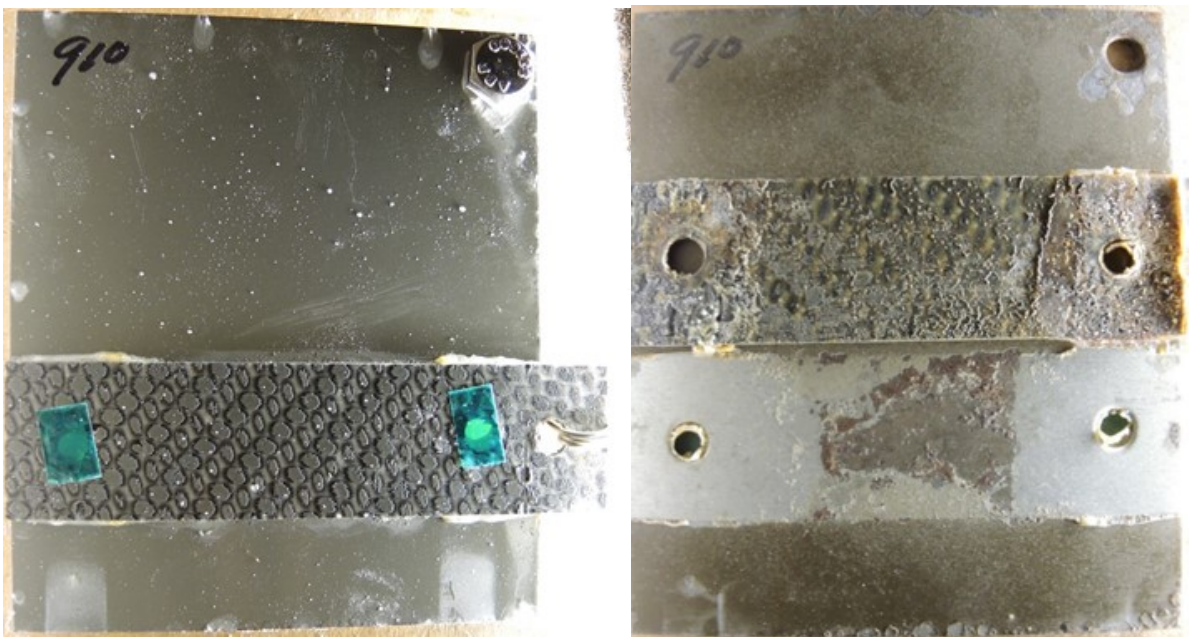

Figure 21. Picture of overlap coupon before and after the top plate was removed.

Some electrocoat deposition deposited in the gap. Red rust was also observed in the gap.

11. Conclusions

This project established the fundamentals of structural adhesive bonding of automotive composites enabling composite-to-metal bonding through the automotive OEM assembly line. Specifically, we have developed understandings on the requirements for surface preparation and adhesive curing for CFRP to produce strong durable structural composite bonds. The specific key findings are listed as follows:

- All joints baked at 145°C are superior to the 180°C counterparts in lap shear performance measured in terms of ultimate strength and displacement to failure.
- The low bake temperature leads to better lap shear performance, which may be attributed to reduced residual stress effect arising from CTE mismatch for dissimilar material joining
- UVO and oxygen plasma treatments were generally effective in improving lap shear performance regardless of oven bake temperatures.
- UVO and oxygen plasma treatments gave quite comparable lap shear performance at 145°C but UVO outperformed plasma at 180°C.
- These findings highlight the importance of surface treatments in promoting adhesion across the interface.

Electrocoat goals for standalone samples were achieved. Additional development is needed to achieve consistency across the various substrates. Additional development is needed for a CFRP panel electrocoat, but this did not prevent obtaining test results for joined panels. All well-known corrosion issues with mixed-material joints were observed. Additional development will address these issues.

PPG will be presenting this work at 2018 Adhesion Society 41st Annual Meeting & 6th World Congress Conference.

12. Recommendations

Further work is needed to complete the development of low-cure adhesives and electrocoat. PPG is working on this development through the DOE project DE-EE0007760 Corrosion Control in Carbon Fiber Reinforced Plastic (CFRP) Composite-Aluminum Closure Panel Hem Joints. Other related IACMI projects are also under consideration.

13. References

BRK Blackman, AJ Kinloch, M Paraschi, WS Teo, *Measuring the mode I adhesive fracture energy, G IC, of structural adhesive joints: the results of an international round-robin*, International journal of adhesion and adhesives, Vol. 23, pp. 293-305, 2003.
JG Williams, End corrections for orthotropic DCB specimens, *Composites Science and Technology*, Vol. 35, pp. 367-376, 1989

14. Appendices

None